Results in Physics 8 (2018) 397–403

Contents lists available at ScienceDirect

Results in Physics

journal homepage: www.journals.elsevier.com/results-in-physics

Flow of 3D Eyring-Powell fluid by utilizing Cattaneo-Christov heat flux model and chemical processes over an exponentially stretching surface

Tanzila Hayat *, S. Nadeem

Department of Mathematics, Quaid-I-Azam University, 45320 Islamabad 44000, Pakistan

ARTICLE INFO

Article history:
Received 21 October 2017
Received in revised form 13 December 2017
Accepted 15 December 2017
Available online 20 December 2017

Keywords:
Three dimensional flow
Eyring-Powell fluid
Cattaneo-Christov heat flux model
Heterogeneous-homogeneous reactions
Exponentially stretching surface

ABSTRACT

This paper examines the three dimensional Eyring-Powell fluid flow over an exponentially stretching surface with heterogeneous-homogeneous chemical reactions. A new model of heat flux suggested by Cattaneo and Christov is employed to study the properties of relaxation time. From the present analysis we observe that there is an inverse relationship between temperature and thermal relaxation time. The temperature in Cattaneo-Christov heat flux model is lesser than the classical Fourier's model. In this paper the three dimensional Cattaneo-Christov heat flux model over an exponentially stretching surface is calculated first time in the literature. For negative values of temperature exponent, temperature profile firstly intensifies to its most extreme esteem and after that gradually declines to zero, which shows the occurrence of phenomenon (SGH) "Sparrow-Gregg hill". Also, for higher values of strength of reaction parameters, the concentration profile decreases.

Introduction

The impact of heat transport phenomenon in liquid flows over a stretching sheet has significant consideration in scientific and technical developments. These developments include rolling the steel at high temperature, metal extrusion, metal working process, paper production, glass fiber production, crystal flowing, and continuous casting. Sakiadis [1] analyzed heat transfer in two dimensional flows past a flat moving sheet. In 1970, Crane [2] continued his work to stretching surface. He analytically analyzed Nusselt number and skin friction. Later on, Wang [3] proposed 3D flow induced by stretching of the surface. Some other applications related to stretching surface may be found in [4–13]. However flow analyses over exponentially stretching sheets are examined sparsely. Magyari and Keller [14] scrutinized the influence of viscous fluid induced by exponentially stretching surface. Elbashbeshy [15] discussed temperature transfer aspects in an exponentially stretching. Khan and Sanjayanand [16] incorporated the study of a second grade over an exponentially stretching surface. Magneto-hydrodynamic thermal boundary layer over an exponentially stretching sheet was analyzed by Al-Odat et al. [17] numerically. Gireesha et al. [18] analyzed Saffman model for magneto-hydrodynamic flow past an exponentially stretching sheet. Further, Nadeem et al. [19] scrutinized impact of radiation in a Jeffrey and viscous liquids past an exponentially stretching sheet. The heat transport phenomenon in a nanofluid flow produced by exponentially stretching sheet was beautifully analyzed by Nadeem and Lee [20].

Most of the liquids including paints, polymer solutions, shampoos, paper pulp, etc., are examples of non-Newtonian. These fluids are applicable in chemical and engineering processes. In non-Newtonian liquids, the relation between flow field and shear stress is complex. On the other hand, the resulting non-linear equations become more complicated due to the viscoelastic characteristics. Most of the scientists are working on the analysis of non-Newtonian fluids. Powell and Eyring [21] incorporated the Eyring-Powell fluid model in 1944. This fluid model is complex in nature but have some aspects instead of other fluids. It is assumed from kinetic theory of fluid instead of empirical expression. Also, it diminishes to viscous fluids for high and low shear rates. This model is utilized to model the manufacturing material flows. The impacts of couple stresses in the characteristic of Eyring-Powell liquid inside the plates were proposed by Eldabe et al. [22]. Zueco and Beg [23] depicts the properties of combine strains using Eyring-Powell fluid model. Islam et al. [24] acquired the perturbation results of the Eyring-Powell liquid. Patel and Timol [25] investigated numerically the characteristics of Eyring-Powell liquid over a wedge. Malik et al. [26] analyzed impacts of variable viscosity using Eyring-Powell liquid. The peristaltic analysis of Eyring-Powell nanofluid was examined by Akbar [27].

* Corresponding author.
E-mail address: t.hayat@math.qau.edu.pk (T. Hayat).

https://doi.org/10.1016/j.rinp.2017.12.038
2211-3797/

The mathematical model proposed by Fourier's (200 years ago) for heat transfer in material is given by $q_i = -k\nabla T_{,i}$, here q_i describes thermal flux vector. The physical interpretation of the Fourier's heat transference is that any preliminary disruption is promptly experienced by medium, which is the major limitation of it. In 1948, Cattaneo [28] overcome this issue, and added thermal relaxation to Fourier's law. Christov [29] further improved the Cattaneo's model. This model is then known as Cattaneo-Christov heat flux model. The phenomenon of heat transfer with thermal convections utilizing Cattaneo heat flux was investigated by Straughan [30,31]. Han et al. [32] explored the slip effects with the Cattaneo-Christov heat flux model using Maxwell fluid. Khan et al. [33] numerically examined the exponentially stretching flow of viscoelastic liquid using the Cattaneo-Christov model. For heterogeneous – homogeneous reactions, the simplest isothermal model was suggested by Chaudhary and Merkin [34]. Khan and Pop [35] numerically explored the 2D stagnation point flow of infinite porous plate with uniform source/sink and homogeneous-heterogeneous reactions. The numerical investigation of viscoelastic liquid with homogeneous-heterogeneous reactions was again investigated by Khan and Pop [36]. Some recent studies on homogeneous-heterogeneous reactions in Eyring-Powell fluid have been presented in [37–40].

In this paper, for the first time, heat flux model for Cattaneo-Christov over an exponentially stretching surface for 3D geometry has been derived. Cattaneo-Christov heat flux model is more generalized form of Fourier's law of heat conduction. Therefore heat flux is analyzed via Cattaneo-Christov heat flux model. Eyring-Powell fluid has been taken into consideration under the stimulus of homogeneous-heterogeneous reactions.

Mathematical modeling and flow analysis

Consider the three-dimensional, incompressible Eyring-Powell liquid flow on an exponentially stretching surface. The laminar flow is restricted in the domain $z > 0$ (see Fig. 1). The velocity components along x and y directions are u_w and v_w respectively. The surface is kept at constant temperature T_w whereas T_∞ being the ambient temperature. A simple model of chemical reactions suggested by Chaudhary and Merkin [34] is considered in the present analysis. The stress tensor $\boldsymbol{\tau}$ is as follows:

$$\boldsymbol{\tau} = -p\boldsymbol{I} + \boldsymbol{\sigma_{ij}}, \tag{1}$$

$$\rho \boldsymbol{a_i} = -\nabla p + \nabla \cdot (\boldsymbol{\sigma_{ij}}), \tag{2}$$

where extra stress tensor is given by

$$\boldsymbol{\sigma_{ij}} = \mu \frac{\partial u_i}{\partial x_j} + \frac{1}{\epsilon}\sinh^{-1}\left(\frac{1}{\delta}\frac{\partial u_i}{\partial x_j}\right), \tag{3}$$

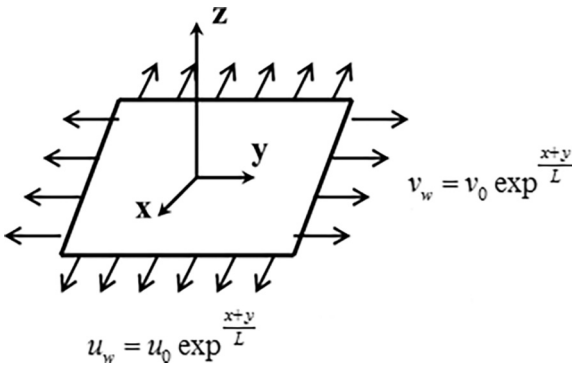

Fig. 1. Physical configuration and coordinate system.

and

$$\sinh^{-1}\left(\frac{1}{\delta}\frac{\partial_i}{\partial x_j}\right) \cong \frac{1}{\delta}\frac{\partial_i}{\partial x_j} - \frac{1}{6}\left(\frac{1}{\delta}\frac{\partial_i}{\partial x_j}\right)^3, \quad \left|\frac{1}{\delta}\frac{\partial_i}{\partial x_j}\right| <<< 1. \tag{4}$$

For three dimensional flow, the principal equations are as follows [25]:

$$\frac{\partial u}{\partial x} + \frac{\partial v}{\partial y} + \frac{\partial w}{\partial z} = 0, \tag{5}$$

$$u\frac{\partial u}{\partial x} + v\frac{\partial u}{\partial y} + w\frac{\partial u}{\partial z} = \left(\nu + \frac{1}{\varepsilon\delta\rho}\right)\frac{\partial^2 u}{\partial z^2} - \frac{1}{2\varepsilon\delta^3\rho}\left(\frac{\partial u}{\partial z}\right)^2\frac{\partial^2 u}{\partial z^2}, \tag{6}$$

$$u\frac{\partial v}{\partial x} + v\frac{\partial v}{\partial y} + w\frac{\partial v}{\partial z} = \left(\nu + \frac{1}{\varepsilon\delta\rho}\right)\frac{\partial^2 v}{\partial z^2} - \frac{1}{2\varepsilon\delta^3\rho}\left(\frac{\partial v}{\partial z}\right)^2\frac{\partial^2 v}{\partial z^2}, \tag{7}$$

$$\rho c_p\left(u\frac{\partial T}{\partial x} + v\frac{\partial T}{\partial y} + w\frac{\partial T}{\partial z}\right) = -\nabla \cdot \vec{q}, \tag{8}$$

$$u\frac{\partial d}{\partial x} + v\frac{\partial d}{\partial y} + w\frac{\partial d}{\partial z} = C_D\frac{\partial^2 d}{\partial z^2} - k_a d e^2, \tag{9}$$

$$u\frac{\partial e}{\partial x} + v\frac{\partial e}{\partial y} + w\frac{\partial e}{\partial z} = C_E\frac{\partial^2 e}{\partial z^2} + k_a d e^2. \tag{10}$$

Here Eyring-Powell fluid properties are denoted by ε and δ and ν, ρ, T, are kinematic viscosity, density and temperature, correspondingly. The diffusion species coefficient are C_D and C_E, respectively. The heat flux $\vec{q}$ satisfies [41]

$$\vec{q} + \lambda_e\left(\frac{\partial \vec{q}}{\partial t} + \vec{V}\cdot\nabla\vec{q} - \vec{q}\cdot\nabla\vec{V} + (\vec{\nabla}\cdot\vec{V})\vec{q}\right) = -\lambda_1\nabla T, \tag{11}$$

The liquid's thermal conductivity and thermal relaxation time is denoted by λ_1 and λ_e, respectively. Replacing $\lambda_e = 0$, Eq. (11) reduced to the Fourier's law. Now eliminate $\vec{q}$ from Eqs. (8) and (11), the following governing equation is as follows [42]:

$$\begin{aligned} u\frac{\partial T}{\partial x} + v\frac{\partial T}{\partial y} + w\frac{\partial T}{\partial z} &= \frac{\lambda_1}{\rho c_p}\frac{\partial^2 T}{\partial z^2} \\ &- \lambda_e\left[u^2\frac{\partial^2 T}{\partial x^2} + v^2\frac{\partial^2 T}{\partial y^2} + w^2\frac{\partial^2 T}{\partial z^2} + 2uv\frac{\partial^2 T}{\partial x\partial y} + 2vw\frac{\partial^2 T}{\partial y\partial z}\right. \\ &+ 2uw\frac{\partial^2 T}{\partial x\partial z} + \left(u\frac{\partial u}{\partial x} + v\frac{\partial u}{\partial y} + w\frac{\partial u}{\partial z}\right)\frac{\partial T}{\partial x} \\ &\left. + \left(u\frac{\partial v}{\partial x} + v\frac{\partial v}{\partial y} + w\frac{\partial v}{\partial z}\right)\frac{\partial T}{\partial y} + \left(u\frac{\partial w}{\partial x} + v\frac{\partial w}{\partial y} + w\frac{\partial w}{\partial z}\right)\frac{\partial T}{\partial z}\right], \end{aligned} \tag{12}$$

With relevant conditions

$$\begin{aligned} &u = u_w,\ v = v_w,\ w = 0,\ T = T_w,\ C_D\frac{\partial d}{\partial z} = k_b d,\ C_E\frac{\partial e}{\partial z} = -k_b d \quad \text{at } z = 0, \\ &u \to 0,\ v \to 0,\ T \to T_\infty,\ d \to d_0\exp^{B\left(\frac{x+y}{2L}\right)},\ e \to 0, \quad \text{as } z \to \infty. \end{aligned} \tag{13}$$

The velocities and temperature at the wall are given by

$$u_w = u_0\exp^{\frac{x+y}{L}}, \quad v_w = v_0\exp^{\frac{x+y}{L}}, \quad T_w = T_\infty + T_0\exp^{A\left(\frac{x+y}{2L}\right)}$$

Now apply the similarity transformations to convert partial differential equations into ordinary differential equations [43]:

$$\eta = \sqrt{\frac{u_0}{2\nu L}}\exp^{\frac{x+y}{2L}} z, \quad u = u_0 \exp^{\frac{x+y}{L}} h'(\eta), \quad v = u_0 \exp^{\frac{x+y}{L}} s'(\eta),$$
$$w = -\sqrt{\frac{\nu u_0}{2L}}\exp^{\frac{x+y}{2L}}(h(\eta) + \eta h'(\eta) + s(\eta) + \eta s'(\eta)),$$
$$T = T_\infty + T_0 \exp^{A\left(\frac{x+y}{2L}\right)} t(\eta), \quad d = d_0 \exp^{B\left(\frac{x+y}{2L}\right)} r(\eta),$$
$$e = d_0 \exp^{B\left(\frac{x+y}{2L}\right)} g(\eta). \tag{14}$$

Here L, A, B and d_0 are reference length, temperature exponent, concentration exponent and positive dimensional constant, respectively.

Eq. (5) is automatically verified and Eqs. (6)–(12) yield

$$(1+\alpha)h''' + (h+s)h'' - 2(h'+s')h' - \alpha\beta(h'')^2 h''' = 0, \tag{15}$$

$$(1+\alpha)s''' + (h+s)s'' - 2(h'+s')s' - \alpha\beta(s'')^2 s''' = 0, \tag{16}$$

$$\frac{1}{\Pr}t'' - A(h'+s')t + (h+s)t' + \frac{\Lambda}{2}[\{\eta(h'+s') + (1+2A)(h+s)\}(h' + s')t' - A\{(A+2)(h'+s')^2 - (h+s)(h''+s'')\}t - (h+s)^2 t''] = 0, \tag{17}$$

$$\frac{1}{Sc}r'' + (h+s)r' - B(h'+s')r - K_1 r g^2 = 0, \tag{18}$$

$$\frac{\Psi}{Sc}g'' + (h+s)g' - B(h'+s')g + K_1 r g^2 = 0, \tag{19}$$

$$h = 0,\ h' = 1,\ s = 0,\ s' = \gamma,\ t = 1,\ r' = k_2 r,$$
$$\Psi g' = -k_2 r, \quad \text{at } \eta = 0,$$
$$h' = 0,\ s' = 0,\ t = 0,\ r = 1,\ g = 0, \quad \text{as } \eta \to \infty, \tag{20}$$

here α, β, Pr, Λ, Sc, K_1, Ψ, γ and K_2 are Eyring-Powell fluid parameters, prandtl number, dimensionless thermal relaxation time, Schmidt number, strength of homogeneous reaction, ratio of diffusion coefficient, stretching ratio parameter and strength of heterogeneous reaction, respectively.

$$\alpha = \frac{1}{\mu\varepsilon\delta},\ \beta = \frac{u_0^3 \exp^{3\left(\frac{x+y}{L}\right)}}{2\nu\delta^2 L},\ Pr = \frac{\upsilon\rho c_p}{\lambda_1},\ \Lambda = \frac{\lambda_e u_0 \exp^{\frac{x+y}{L}}}{L},$$
$$Sc = \frac{\upsilon}{C_D},\ K_1 = \frac{k_a d_0^2}{2u_0 L}\exp^{(B+1)\left(\frac{x+y}{L}\right)},\ \Psi = \frac{C_E}{C_D},\ \gamma = \frac{v_0}{u_0},$$
$$K_2 = \frac{k_b}{C_D}\sqrt{\frac{2\upsilon L}{u_0}}\exp^{-\left(\frac{x+y}{2L}\right)} \tag{21}$$

It is assume that diffusion coefficients of D and E species are of comparable size, which means that C_D and C_E are equal which implies $\Psi = 1$. Therefore

$$r + g = 1. \tag{22}$$

So Eqs. (18)–(19) takes the following form as

$$\frac{1}{Sc}r'' + (h+s)r' - B(h'+s')r - K_1 r(1-r)^2 = 0, \tag{23}$$

and

$$r'(0) = K_2 r(0), \quad r(\infty) \to 1. \tag{24}$$

For engineering interest, C_f is demarcated as

$$C_f = \frac{\sigma_w}{\rho u_w^2}, \tag{25}$$

where the wall shear stress σ_w is given by

$$\sigma_w = \left(\mu + \frac{1}{\varepsilon\delta}\right)\frac{\partial u}{\partial z}\bigg|_{z=0} - \frac{1}{6\varepsilon\delta^3}\left(\frac{\partial u}{\partial z}\right)^3\bigg|_{z=0}, \tag{26}$$

or

$$\sqrt{2\,\mathrm{Re}}C_f = (1+\alpha)h''(0) - \frac{\alpha\beta}{3}(h''(0))^3. \tag{27}$$

Numerical process

The set of highly non-linear and coupled ordinary differential equations i.e. Eqs. (15)–(17) and (23) along with boundary conditions (20) and (24) are solved numerically by utilizing a solution method named BVP-4C [44,45] in MATLAB software. Firstly, the governing ODEs (15)–(17) and (23) have been converted into first order ODEs because this solution method is applicable for first order initial value problems only.

$$y_1 = h, \quad y_2 = h', \quad y_3 = h'', \quad y_4 = s, \quad y_5 = s',$$
$$y_6 = s'', \quad y_7 = t, \quad y_8 = t', \quad y_9 = r, \quad y_{10} = r', \tag{28}$$

$$y_1' = y_2 \tag{29}$$

$$y_2' = y_3 \tag{30}$$

$$y_3' = \frac{1}{[1+\alpha-\alpha\beta y_3^2]}[2(y_2+y_5)y_2 - (y_1+y_4)y_3] \tag{31}$$

$$y_4' = y_5 \tag{32}$$

$$y_5' = y_6 \tag{33}$$

$$y_6' = \frac{1}{[1+\alpha-\alpha\beta y_6^2]}[2(y_2+y_5)y_5 - (y_1+y_4)y_6] \tag{34}$$

$$y_7' = y_8 \tag{35}$$

$$y_8' = \frac{1}{\left[\frac{1}{\Pr} - \frac{\Lambda}{2}(y_1+y_4)^2\right]}[A(y_2+y_5)y_7 - (y_1+y_4)y_8 - \frac{\Lambda}{2}[\{\eta(y_2+y_5) + (1+2A)(y_1+y_4)\}(y_2+y_5)y_8 - A\{(A+2)(y_2+y_5)^2 - (y_1+y_4)(y_3+y_6)\}y_7]] \tag{36}$$

$$y_9' = y_{10} \tag{37}$$

$$y_{10}' = Sc[B(y_2+y_5)y_9 - (y_1+y_4)y_{10} - k_1(1-y_9)^2 y_9] \tag{38}$$

With relevant initial conditions

$$y_1(0) = 0, \quad y_2(0) = 1, \quad y_4(0) = 0, \quad y_5(0) = \gamma,$$
$$y_7(0) = 1, \quad y_{10}(0) - k_2 y_9(0) = 0, \tag{39}$$

From the above system, there are ten equations and six initial conditions. Therefore, the appropriate initial guesses are chosen for $y_3(0)$, $y_6(0)$, $y_8(0)$, and $y_{10}(0)$. The criteria for the solution to converge were set to 10^{-6}. The procedure was revised until the required criterion was achieved.

Discussion section

In this segment, the effect of relevant physical parameters i.e. Eyring-Powell fluid parameter α, stretching ratio parameter γ, temperature exponent A, thermal relaxation time Λ, Prandtl number Pr, concentration exponent B, chemical reactions K_1, K_2 and Schmidt number Sc on velocities along x and y directions, temperature and concentration distributions are represented in graphical and tabular form.

Fig. 2 describe the behavior of Eyring-Powell liquid parameter α, on all velocity profiles $h'(\eta)$ and $s'(\eta)$. This model explains the properties of shear thinning liquid. From Fig. 2, as the Eyring-Powell fluid parameter α increases, the velocity component also increases.

Fig. 3 portrays the impacts of stretching ratio parameter γ on h' and s' distributions. One can notice that intensification in γ prompts reducing h' distribution but an opposite trend is observed for s' profile. In fact the stretching rate along y direction is higher because the adjacent surface starts to move in that direction rather than x direction. Due to this reason, h' profile decreases while s' profile increases.

Fig. 4 elucidates temperature exponent A impacts on temperature profile t for both positive and negative values of temperature exponent A. For any under consideration value of A, there is a decrease in temperature distribution t.

Fig. 5 portrays the impacts of Eyring-Powell fluid parameter α on temperature distribution. From figure, temperature and thermal boundary layer thickness are decreasing functions of Eyring-Powell fluid parameter α.

In Fig. 6, temperature distribution is plotted for various values of non-dimensional relaxation time Λ. It is noticed that there is an inverse relationship between temperature and thermal relaxation time. As $\Lambda = 0$ relates to traditional Fourier's law, therefore it can be concluded that in Cattaneo-Christov heat flux model, temperature is lesser than the classical Fourier's model.

Fig. 7 elucidates stretching ratio parameter γ impacts on temperature profile t for both positive and negative values of temperature exponent A. For any under consideration value of A, there is a decrease in temperature distribution t as stretching ratio parame-

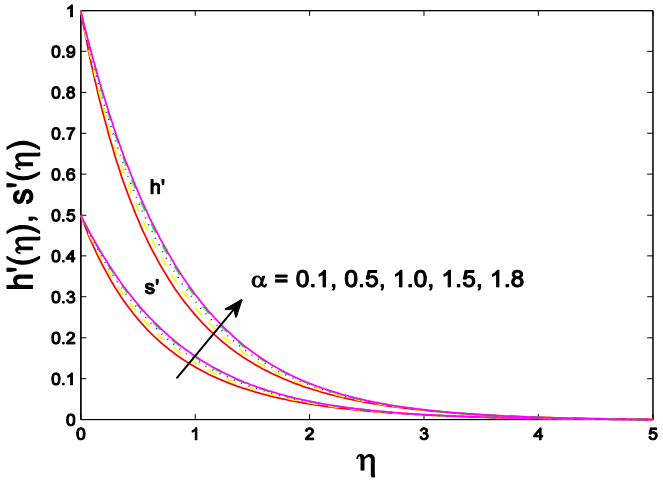

Fig. 2. Impact of α on $h'(\eta)$ and $s'(\eta)$.

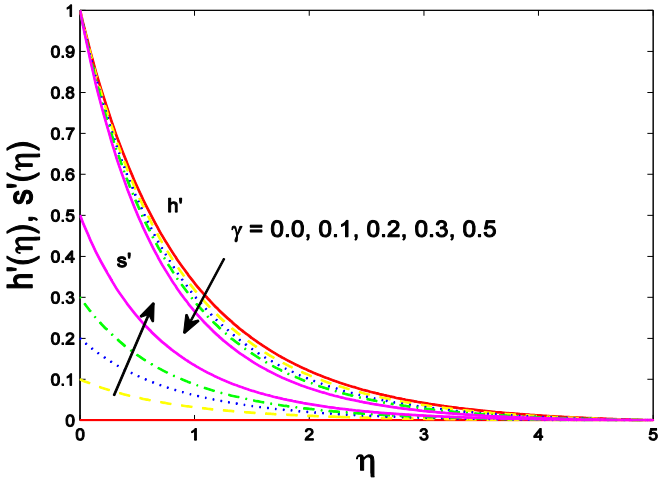

Fig. 3. Impact of γ on $h'(\eta)$ and $s'(\eta)$.

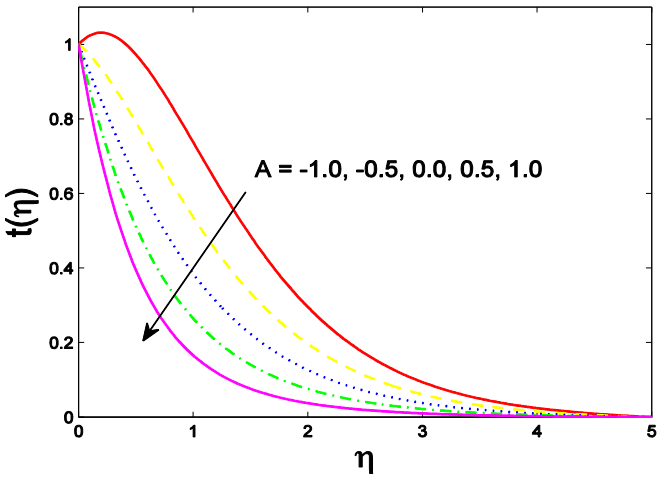

Fig. 4. Impact of A on $t(\eta)$.

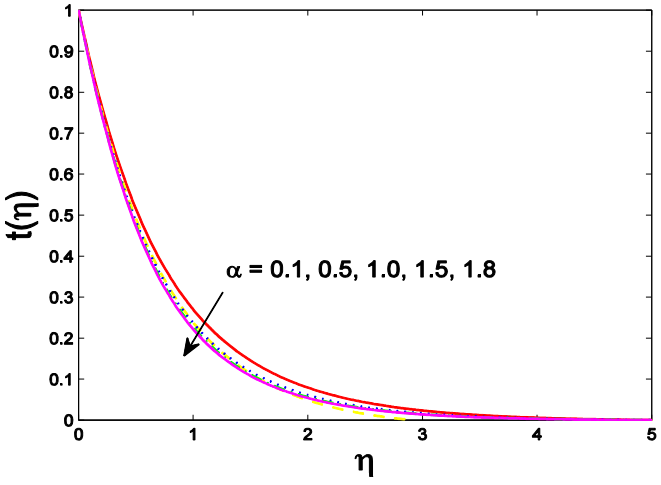

Fig. 5. Impact of α on $t(\eta)$.

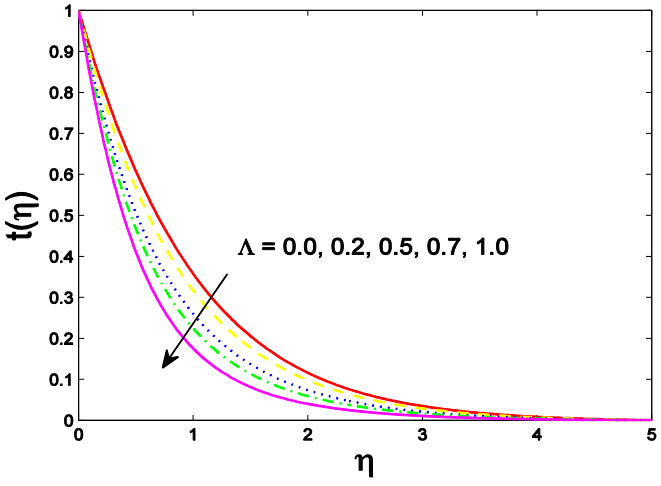

Fig. 6. Impact of Λ on $t(\eta)$.

ter γ increases. For negative A, temperature profile firstly intensifies to its most extreme esteem and after that gradually declines to zero, which shows the occurrence of phenomenon (SGH) "Sparrow-Gregg hill". From this figure, for positive A, the temperature distribution t near the wall is concave upward and for negative A, temperature distribution is concave down. Also, as γ increases, the thicknesses of thermal boundary declines. This finding is in a good settlement with the outcomes of Laha et al. [4] for the 3D problem over a linearly stretching surface.

Fig. 8 illustrates the impacts of Pr on $t(\eta)$. Physically, the relation between Prandtl and thermal diffusivity is inverse. As Prandtl number Pr increases, one can expect that there are less thermal impacts to infiltrate into the liquid. Consequently, as increase in Pr, the temperature and corresponding thermal layer thickness decreases.

Fig. 9 describes the effects of concentration exponent B on concentration profile r. From figure it is notice that the influence of concentration exponent B on $r(\eta)$ is decreasing.

Impact of stretching ratio parameter γ on $r(\eta)$ is analyzed in Fig. 10. By the intensification of γ, for any under consideration value of concentration exponent B, the concentration distribution increases. This is due to the increment of stretching along y direction that is why concentration enhances.

Fig. 11 shows the influence of Eyring-Powell fluid parameter α on concentration profile r. It is observed from this figure that impact of Eyring-Powell fluid parameter α on $r(\eta)$ is increasing.

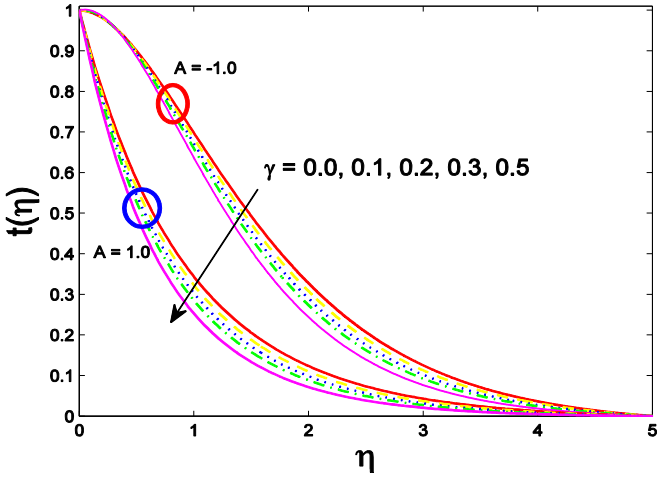

Fig. 7. Impact of γ on $t(\eta)$.

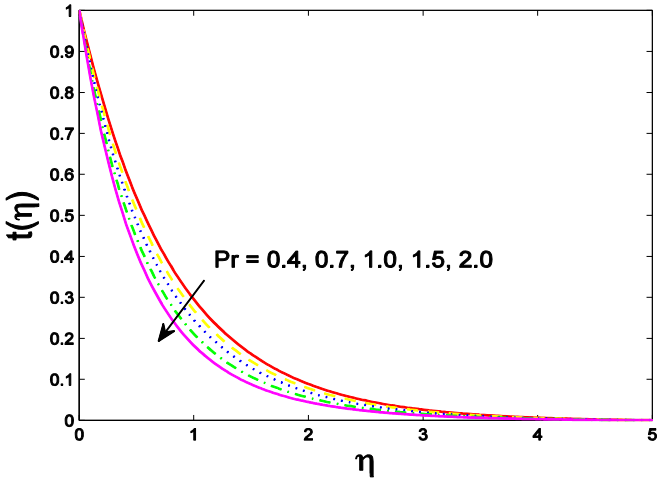

Fig. 8. Impact of Pr on $t(\eta)$.

The effects of homogeneous reaction parameter K_1 and heterogeneous reaction parameter K_2 on concentration distribution are depicted in Figs. 12 and 13. With an increase in K_1 and K_2, the concentration profiles depreciates. It may be the domination of

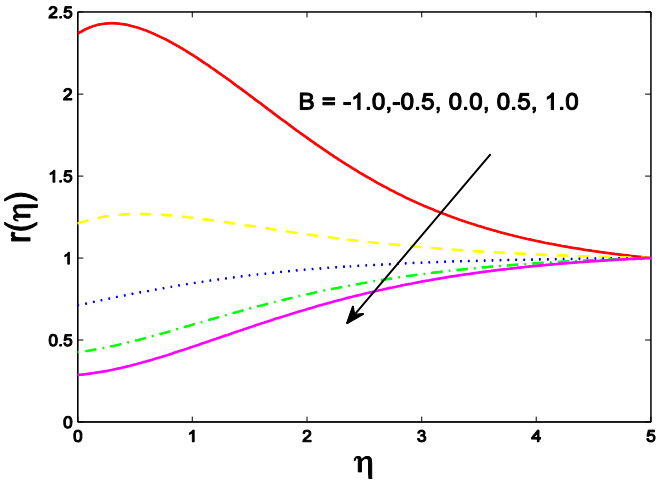

Fig. 9. Impact of B on $r(\eta)$.

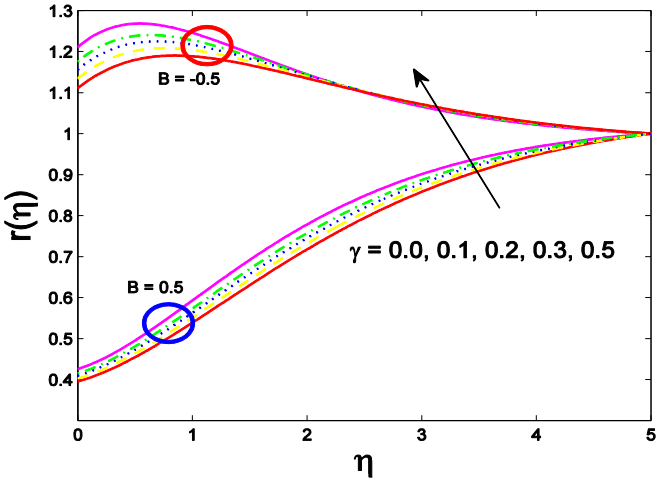

Fig. 10. Impact of γ on $r(\eta)$.

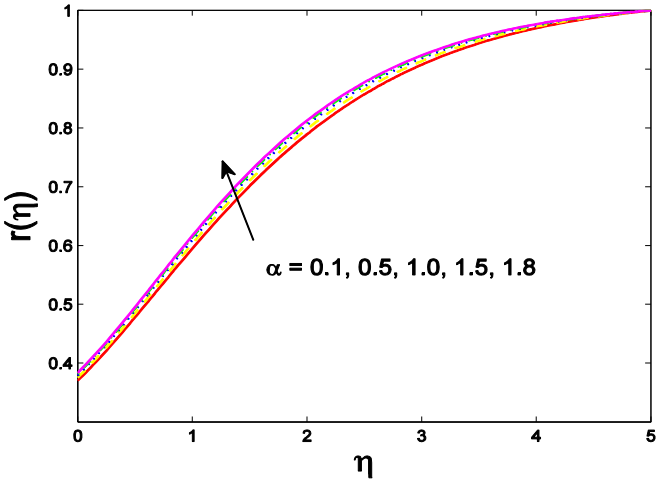

Fig. 11. Impact of α on $r(\eta)$.

diffusion coefficient than reaction rate. This shows the good agreement with Raju et al. [46].

Fig. 14 elucidates the variation of Schmidt number Sc on concentration field. For larger values of Schmidt number Sc, the increasing behavior of concentration profile r is observed.

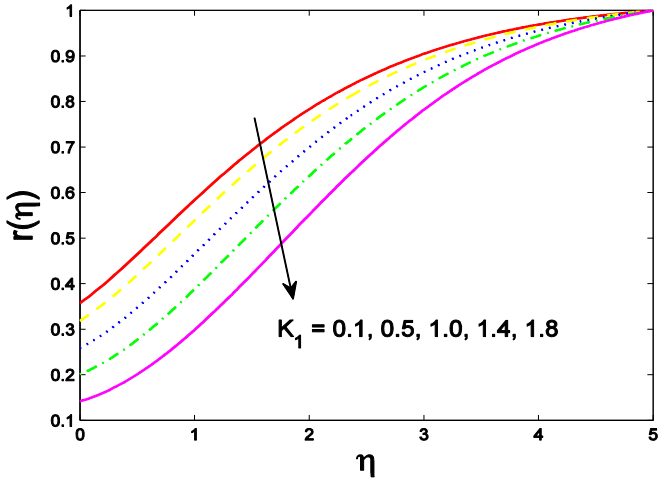

Fig. 12. Impact of K_1 on $r(\eta)$.

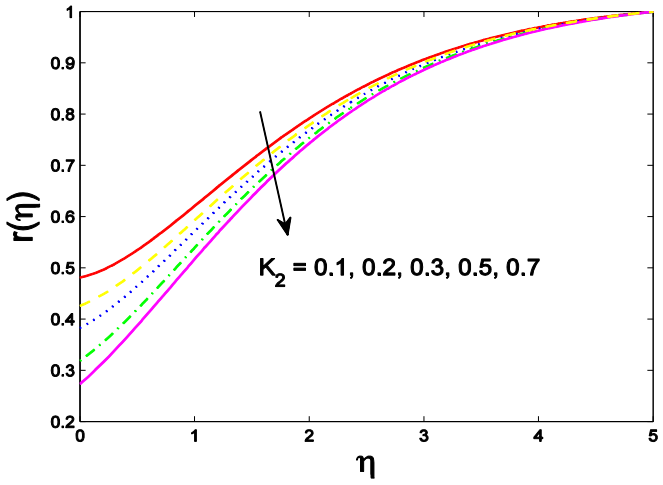

Fig. 13. Impact of K_2 on $r(\eta)$.

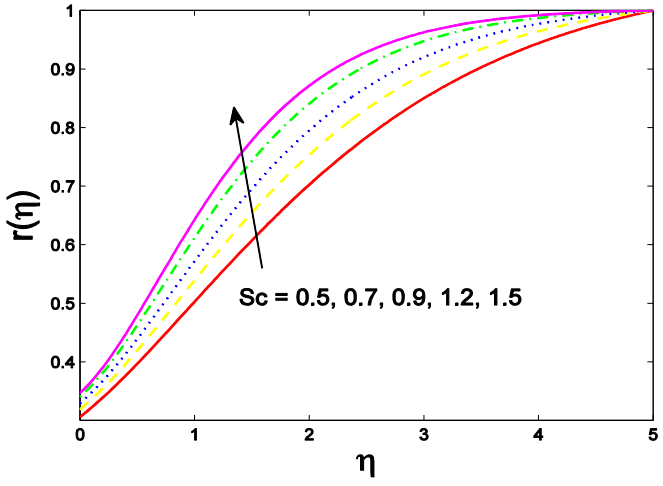

Fig. 14. Impact of Sc on $r(\eta)$.

Physically, increasing values of Sc relate to high rate of viscous diffusion which causes the concentration of a fluid to increase.

Figs. 15–16 are sketched to see the influence of Eyring-Powell fluid parameter α on the shear stress versus stretching ratio parameter γ. These figures reveals that the flow resistance increments with the variation of Eyring-Powell fluid parameter α as well as with stretching ratio parameter γ, therefore, shear stress increases in both directions. From Table 1, the magnitude of skin friction increments with an expansion in α and γ. However it reduces when β increases.

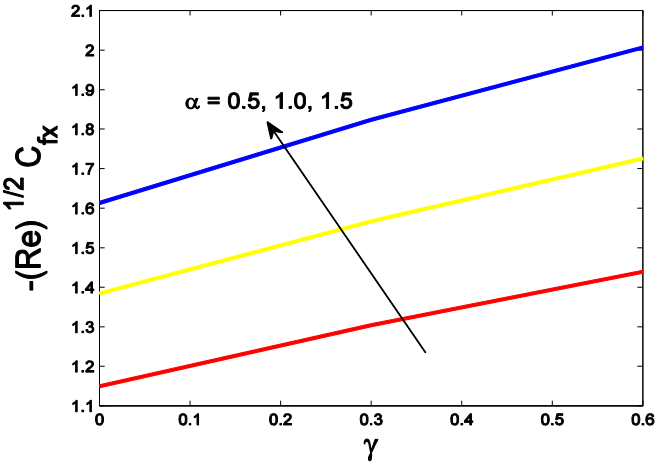

Fig. 15. Impact of α on skin friction along x direction.

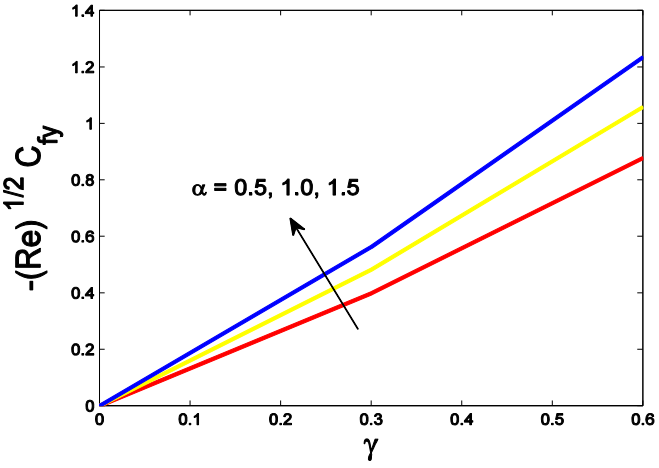

Fig. 16. Impact of α on skin friction along y direction.

Table 1
Effects of skin friction C_f along x and y directions.

α	β	γ	$C_{fx}(Re)^{\frac{1}{2}}$	$C_{fy}Re^{\frac{1}{2}}$
0.1	0.3	0.5	−1.16824	−0.586858
0.5			−1.39662	−0.709678
1.0			−1.67553	−0.85724
1.5			−1.94891	−1.00084
1.8			−2.11098	−1.08575
0.3	0.1	0.5	−1.29827	−0.651541
	0.2		−1.29077	−0.650262
	0.3		−1.28308	−0.648959
	0.5		−1.2670	−0.646263
	0.6		−1.25854	−0.644862
0.3	0.3	0.0	−1.05405	0.0
		0.1	−1.10412	−0.111621
		0.2	−1.15183	−0.233044
		0.3	−1.19743	−0.363538
		0.5	−1.28309	−0.648961

Concluding remarks

The three dimensional Eyring-Powell fluid flow using Cattaneo-Christov heat flux model and heterogeneous-homogeneous chemical reactions over an exponentially stretching surface was intended to investigate in this paper. The governing nonlinear partial differential equations are transformed into strong nonlinear ordinary differential equations using similarity transformations. The nonlinear ordinary differential equations along with boundary conditions are tackled numerically by using bvp-4c technique. From the presented study, the following conclusions were drawn:

- The intensification in stretching ratio parameter γ prompts reducing h' distribution but an opposite trend is observed for s' profile.
- Temperature in Cattaneo-Christov heat flux model is lesser as compared to classical Fourier's model.
- There is a decrease in temperature distribution t as stretching ratio parameter γ increases.
- For negative values of temperature exponent A, temperature profile shows the occurrence of phenomenon (SGH) "Sparrow-Gregg hill".
- By the intensification of γ, for under consideration value of concentration exponent B, the concentration distribution increases.
- The flow resistance increments with the variation of α as well as with γ,therefore, shear stress increases.

References

[1] Sakiadis BC. Boundary-layer behavior on continuous solid surfaces: I. Boundary layer equations for two-dimensional and axisymmetric flow. AIChE J 1961;7:26–8. also see part II, 221–5.
[2] Crane LJ. Flow past a stretching plate. Zeitschrift für angewandte Mathematik und Physik (ZAMP) 1970;21(4):645–7.
[3] Wang CY. The three-dimensional flow due to a stretching flat surface. Phys Fluids 1984;27(8):1915–7.
[4] Laha MK, Gupta PS, Gupta AS. Heat transfer characteristics of the flow of an incompressible viscous fluid over a stretching sheet. Heat Mass Transfer 1989;24(3):151–3.
[5] Hsiao KL. To promote radiation electrical MHD activation energy thermal extrusion manufacturing system efficiency by using Carreau-Nanofluid with parameters control method. Energy 2017;130:486–99.
[6] Hsiao KL. Combined electrical MHD heat transfer thermal extrusion system using Maxwell fluid with radiative and viscous dissipation effects. Appl Therm Eng 2017;112:1281–8.
[7] Hsiao KL. Micropolar nanofluid flow with MHD and viscous dissipation effects towards a stretching sheet with multimedia feature. Int J Heat Mass Transfer 2017;112:983–90.
[8] Hsiao KL. Stagnation electrical MHD nanofluid mixed convection with slip boundary on a stretching sheet. Appl Therm Eng 2016;98:850–61.
[9] Hsiao KL. Numerical solution for Ohmic Soret-Dufour heat and mass mixed convection of viscoelastic fluid over a stretching sheet with multimedia physical features. J Aerosp Eng 2016;30(1):04016082.
[10] Hayat T, Nadeem S. Induced magnetic field stagnation point flow of nanofluid past convectively heated stretching sheet with Buoyancy effects. Chin Phys B 2016;25(11):114701.
[11] Ishak A, Jafar K, Nazar R, Pop I. MHD stagnation point flow towards a stretching sheet. Physica A 2009;388(17):3377–83.
[12] Hayat T, Nadeem S. The effects of MHD and buoyancy on Hematite water-based fluid past a convectively heated stretching sheet. Neural Comput Appl 2017:1–8.
[13] Hayat T, Nadeem S. Heat transfer enhancement with Ag–CuO/water hybrid nanofluid. Results Phys 2017;7:2317–24.
[14] Magyari E, Keller B. Heat and mass transfer in the boundary layers on an exponentially stretching continuous surface. J Phys D Appl Phys 1999;32(5):577.
[15] Elbashbeshy EMA. Heat transfer over an exponentially stretching continuous surface with suction. Arch Mech 2001;53(6):643–51.
[16] Khan SK, Sanjayanand E. Viscoelastic boundary layer flow and heat transfer over an exponential stretching sheet. Int J Heat Mass Transfer 2005;48(8):1534–42.
[17] Damseh R. Thermal boundary layer on an exponentially stretching continous surface in the presence of magnetic field effect. Int J Appl Mech Eng 2006;11(2):289–99.
[18] Gireesha BJ, Pavithra GM, Bagewadi CS. Boundary layer flow and heat transfer of a dusty fluid over an exponentially stretching sheet. British J Math Comput Sci 2012;2(4):187–97.
[19] Nadeem S, Zaheer S, Fang T. Effects of thermal radiation on the boundary layer flow of a Jeffrey fluid over an exponentially stretching surface. Numer Algorithms 2011;57(2):187–205.
[20] Nadeem S, Lee C. Boundary layer flow of nanofluid over an exponentially stretching surface. Nanoscale Res Lett 2012;7(1):94.
[21] Powell RE, Eyring H. Mechanism for relaxation theory of viscosity. Nature 1944;154(55):427–8.
[22] Eldabe NTM, Hassan AA, Mohamed MA. Effect of couple stresses on the MHD of a non-Newtonian unsteady flow between two parallel porous plates. Zeitschrift für Naturforschung A 2003;58(4):204–10.
[23] Zueco J, Bég OA. Network numerical simulation applied to pulsatile non-Newtonian flow through a channel with couple stress and wall mass flux effects. Int J Appl Math Mech 2009;5(2):1–16.
[24] Islam S, Shah A, Zhou CY, Ali I. Homotopy perturbation analysis of slider bearing with Powell-Eyring fluid. Zeitschrift für Angewandte Mathematik und Physik (ZAMP) 2009;60(6):1178–93.
[25] Patel M, Timol MG. Numerical treatment of Powell-Eyring fluid flow using method of satisfaction of asymptotic boundary conditions (MSABC). Appl Numer Math 2009;59(10):2584–92.
[26] Malik MY, Bilal S, Bibi M, Ali U. Logarithmic and parabolic curve fitting analysis of dual stratified stagnation point MHD mixed convection flow of Eyring-Powell fluid induced by an inclined cylindrical stretching surface. Results Phys 2017;7:544–52.
[27] Akbar NS. Application of Eyring-Powell fluid model in peristalsis with nano particles. J Comput Theor Nanosci 2015;12(1):94–100.
[28] Cattaneo C. Sulla conduzione del calore. Atti Sem. Mat. Fis. Univ. Modena 1948;3:83–101.
[29] Christov CI. On frame indifferent formulation of the Maxwell-Cattaneo model of finite-speed heat conduction. Mech Res Commun 2009;36(4):481–6.
[30] Straughan B. Stability and wave motion in porous media, vol. 165. New York: Springer; 2008. p. xiv+-437.
[31] Straughan B. Thermal convection with the Cattaneo-Christov model. Int J Heat Mass Transfer 2010;53(1):95–8.
[32] Han S, Zheng L, Li C, Zhang X. Coupled flow and heat transfer in viscoelastic fluid with Cattaneo-Christov heat flux model. Appl Math Lett 2014;38:87–93.
[33] Khan JA, Mustafa M, Hayat T, Alsaedi A. Numerical study of Cattaneo-Christov heat flux model for viscoelastic flow due to an exponentially stretching surface. PLoS One 2015;10(9):e0137363.
[34] Chaudhary MA, Merkin JH. A simple isothermal model for homogeneous-heterogeneous reactions in boundary-layer flow. I Equal diffusivities. Fluid Dyn Res 1995;16(6):311–33.
[35] Khan WA, Pop I. Flow near the two-dimensional stagnation-point on an infinite permeable wall with a homogeneous–heterogeneous reaction. Commun Nonlinear Sci Numer Simul 2010;15(11):3435–43.
[36] Khan WA, Pop IM. Effects of homogeneous–heterogeneous reactions on the viscoelastic fluid toward a stretching sheet. J Heat Transfer 2012;134(6):064506.
[37] Hayat T, Imtiaz M, Alsaedi A. Effects of homogeneous-heterogeneous reactions in flow of Powell-Eyring fluid. J Central South University 2015;22(8):3211–6.
[38] Khan NA, Sultan F. Homogeneous-heterogeneous reactions in an Eyring-Powell fluid over a stretching sheet in a porous medium. Spec Top Rev Porous Media: Int J 2016;7(1).
[39] Khan I, Malik MY, Salahuddin T, Khan M, Rehman KU. Homogenous–heterogeneous reactions in MHD flow of Powell-Eyring fluid over a stretching sheet with Newtonian heating. Neural Comput Appl 2017:1–8.
[40] Hayat T, Nadeem S. Aspects of developed heat and mass flux models on 3D flow of Eyring-Powell fluid. Results Phys 2017;7:3910–7.
[41] Tibullo V, Zampoli V. A uniqueness result for the Cattaneo-Christov heat conduction model applied to incompressible fluids. Mech Res Commun 2011;38(1):77–9.
[42] Dong Y, Cao BY, Guo ZY. Generalized heat conduction laws based on thermomass theory and phonon hydrodynamics. J Appl Phys 2011;110(6):063504.
[43] Liu IC, Wang HH, Peng YF. Flow and heat transfer for three-dimensional flow over an exponentially stretching surface. Chem Eng Commun 2013;200(2):253–68.
[44] Shampine LF, Gladwell I, Thompson S. Solving ODEs with matlab. Cambridge University Press; 2003.
[45] Shampine LF, Kierzenka J, Reichelt MW. Solving boundary value problems for ordinary differential equations in MATLAB with bvp4c. Tutorial Notes 2000;2000:1–27.
[46] Raju CSK, Sandeep N, Saleem S. Effects of induced magnetic field and homogeneous–heterogeneous reactions on stagnation flow of a Casson fluid. Eng Sci Tech, Int J 2016;19(2):875–87.